High spatial resolution distributed sensing in optical fibers by Brillouin gain-profile tracing

Tom Sperber,[1,*] Avishay Eyal,[1] Moshe Tur,[1] and Luc Thévenaz[2]

[1]School of Electrical Engineering, Faculty of Engineering, Tel-Aviv University, Tel-Aviv 69978, Israel
[2]Ecole Polytechnique Fédérale de Lausanne, Institute of Electrical Engineering, STI-GR-SCI Station 11, CH-1015
Lausanne, Switzerland
*tomsperb@post.tau.ac.il

Abstract: A novel BOTDA technique for distributed sensing of the Brillouin frequency in optical fibers with cm-order spatial resolution is proposed. The technique is based upon a simple modulation scheme, requiring only a single long pump pulse for acoustic excitation, and no subsequent interrogating pulse. Instead, the desired spatial mapping of the Brillouin response is extracted by taking the derivative of the probe signal. As a result, the spatial resolution is limited by the fall-time of the pump modulation, and the phenomena of secondary "echo" signals, typically appearing in BOTDA sensing methods based upon pre-excitation, is mitigated. Experimental demonstration of the detection of a Brillouin frequency variation significantly smaller than the natural Brillouin linewidth, with a 2cm spatial resolution, is presented.

©2010 Optical Society of America

OCIS codes: (060.2370) Fiber optics sensors; (290.5900) Scattering, stimulated Brillouin; (350.5730) Resolution.

References and links

1. L. Zou, X. Bao, Y. Wan, and L. Chen, "Coherent probe-pump-based Brillouin sensor for centimeter-crack detection," Opt. Lett. **30**(4), 370–372 (2005).
2. A. W. Brown, B. G. Colpitts, and K. Brown, "Dark-pulse Brillouin optical time-domain sensor with 20-mm spatial resolution," J. Lightwave Technol. **25**(1), 381–386 (2007).
3. Y. Koyamada, Y. Sakairi, N. Takeuchi, and S. Adachi, "Novel technique to improve spatial resolution in Brillouin optical time-domain reflectometry," IEEE Photon. Technol. Lett. **19**(23), 1910–1912 (2007).
4. L. Thévenaz, and S. F. Mafang, "Distributed fiber sensing using Brillouin echoes," Proc. SPIE **7004**, 1–4 (2008).
5. W. Li, X. Bao, Y. Li, and L. Chen, "Differential pulse-width pair BOTDA for high spatial resolution sensing," Opt. Express **16**, 16–25 (2008).
6. V. Lecoeuche, D. J. Webb, C. N. Pannell, and D. A. Jackson, "Transient response in high-resolution Brillouin-based distributed sensing using probe pulses shorter than the acoustic relaxation time," Opt. Lett. **25**(3), 156–158 (2000).
7. H. Naruse, and M. Tateda, "Trade-off between the spatial and the frequency resolutions in measuring the power spectrum of the Brillouin backscattered light in an optical fiber," Appl. Opt. **38**(31), 6516–6521 (1999).
8. R. W. Boyd, *Nonlinear Optics,* 2nd. ed.(Academic Press, 2003), Chap. 9.
9. M. Nikles, L. Thévenaz, and P. A. Robert, "Brillouin gain spectrum characterization in single-mode optical fibers," J. Lightwave Technol. **15**(10), 1842–1851 (1997).

1. Introduction

Distributed strain and temperature sensing in optical fibers using Stimulated Brillouin Scattering (SBS) has been developing recently in various beneficial aspects. Particularly, much attention has been drawn to the objective of improving the sensors' spatial resolution, and several researchers have proposed and investigated novel techniques which bring this resolution into the single-centimeter range [1–5]. The common working principle shared by all the novel techniques is the optically-induced pre-excitation of an acoustic wave in the sensing medium, prior to the actual measurement process. This eliminates the problem which limits the conventional Brillouin Optical Time-Domain Analysis (BOTDA) scheme's resolution, namely - the broadening and lowering of the Brillouin gain spectrum as the temporal duration of the pumping pulse is reduced to values comparable with the acoustic

relaxation time [6]. Since the conventional scheme employs the pump pulse as both the generator of the SBS gain process and as the instrument used to sense it, the attempt to improve spatial resolution by shortening the pump pulse diminishes the strength and the spectral selectiveness of the acoustic response, thus degrading the frequency resolution and the SNR of the sensor [7]. Contrastingly, the novel high-resolution techniques detach the role of "writing" the information from that of "reading" it, by employing a pre-pump as the builder of SBS response, and then interrogating the response separately. This removes any constraints relating the duration of the interrogating pulse to the acoustic lifetime.

The BOTDA sensing method proposed in this paper relies on pre-excitation of the acoustic field in the fiber, much like the techniques mentioned above, but differs in the way the measurement itself is performed and interpreted. The method can be briefly described in the following manner: First, steady-state continuous-wave (CW) Brillouin gain is generated throughout the sensing fiber, and then, following the abrupt shut-down of the pump, the probe power is monitored in the time domain. As shall be corroborated in this paper both theoretically and experimentally, the derivative of the signal thus obtained directly represents the spatial profile of the Brillouin gain along the fiber.

2. Working Principle of Method

During the pre-excitation phase, probe light propagating through the fiber experiences SBS amplification at any point characterized by a "tuned" local Brillouin frequency, i.e., one that matches the pump-probe frequency difference. The way the probe's power evolves along its path (this we shall from here on refer to as the "gain profile") is unknown to us, for we detect only its integral result upon the probe power at the fiber end. Supposing, however, we were to nullify the gain occurring over the last centimeter of the fiber, while leaving the situation everywhere else as is; The difference between the power detected in this state and the power detected previously, would represent the gain contributed only by the last cm (as visualized in Fig. 1). By repeating this differential process from fiber end to beginning, we could reveal the complete gain profile of the probe. This measurement process is easily realized by rapidly switching off the pump power: The falling edge function for the pumping field traverses the fiber from its end to its beginning, and the Brillouin gain gradually vanishes with it.
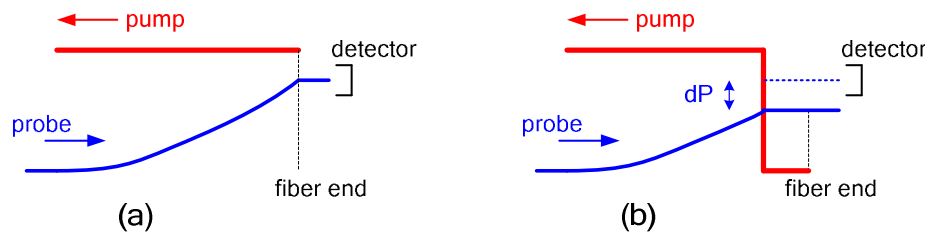

Fig. 1. Schematic illustration of the SBS gain profiles experienced by the probe light, for: (a) pump power exists along the entire length of the fiber, and (b) pump power drops to zero in the last section of fiber only. The gain which occurred along this section in situation (a) is detected in situation (b) as the difference dP.

The essential idea behind this approach is that once pre-excitation SBS has been induced, no need arises for an interrogation pulse which actually backscatters upon the acoustic waves. Instead, one can simply extinguish the pump, trace the gain profile the probe has undergone during the pre-pumping, and deduce the desired information through elementary signal processing. This technique shall be from here on identified as "Gain-Profile Tracing" (GPT).

3. Theory

We formulate the Brillouin interaction between the pumping laser beam, and the counter-propagating Stokes light, through these scalar coupled wave equations [8]:

$$\frac{\partial E_p}{\partial z} - \frac{1}{v_g}\frac{\partial E_p}{\partial t} = -j\frac{\gamma_e \omega_p}{4\rho_0 nc}E_s \cdot \rho - \alpha E_p \qquad (1)$$

$$\frac{\partial E_s}{\partial z} + \frac{1}{v_g}\frac{\partial E_s}{\partial t} = j\frac{\gamma_e \omega_s}{4\rho_0 nc}E_p \cdot \rho * - \alpha E_s \qquad (2)$$

$$\frac{\partial \rho}{\partial t} + \left[\frac{\Gamma_B}{2} - j(\Omega_B - \omega_p + \omega_s)\right]\rho = j\frac{\gamma_e \Omega_B}{8\pi v_a^2}E_p \cdot E_s * \qquad (3)$$

Here E_p, E_s, ρ stand for the complex amplitudes of the pump field, the Stokes field, and the acoustic wave, respectively. ω_p, ω_s are the optical frequencies of the pump and Stokes lightwaves, Ω_B is the Brillouin frequency, Γ_B is the Brillouin natural linewidth, v_a is the acoustic velocity in the fiber, γ_e is the electrostrictive constant, and lastly n, v_g, ρ_0, α are the refractive index, optical group velocity, density, and attenuation coefficient of the fiber. We make two approximations common in the literature: First, considering the case of a weak Stokes light (compared to the power of the pumping beam), we assume the latter remains non-depleted throughout the fiber. Second, we omit the constant fiber loss, which is negligible over the rather short propagation distances typical to the working regime of high-resolution sensing. Now, if the two counter-propagating lightwaves are launched into the fiber as CWs, after a time sufficiently long for the SBS process to reach steady-state amplification, the build-up of the power of the Stokes light along the Brillouin interaction length is described by the following differential equation [8]:

$$\frac{dP_s(z)}{dz} = GI_p \cdot P_s(z) \quad where \quad G(z, \omega_p - \omega_s) = \frac{\gamma_e^2 \omega_s^2}{nc^3 v_a \rho_0 \Gamma_B} \cdot \frac{(\Gamma_B/2)^2}{(\Omega_B - \omega_p + \omega_s)^2 + (\Gamma_B/2)^2} \qquad (4)$$

Here P_s represents the probe (Stokes) power. The Brillouin gain is proportional to the intensity of the pump light, denoted I_p, and the Brillouin gain coefficient $G(z, \omega)$, which has dimensions of m/W. For fixed pump and probe optical frequencies, G becomes a function of location only, and Eq. (4) is readily solved thus:

$$P_s(z) = P_{s0} \exp\left[\int_0^z I_p G(z')dz'\right] \qquad (5)$$

Here P_{s0} is the probe power initially injected into the fiber at $z = 0$. We are interested in the Stokes power observed by the photodetector placed at the end of the interaction length, namely at $z = L$. Now we assume the pump power is switched off at the fiber end at some moment $t = 0$, and consider the dynamics immediately following. The pump field in the fiber can be viewed as step-function with its falling edge propagating towards $z = 0$. At any point where $E_p = 0$, the source terms in both Eq. (2) and Eq. (3) are nullified, and the SBS process instantaneously vanishes – regardless of the slow relaxation time of the acoustic phonons. Hence, for any later moment $t > 0$, the Stokes wave front currently passing the pump pulse's falling edge (at $L - v_g t$), will incur significant amplification only along the interval $0 \le z \le L - v_g t$. Provided that any effect of the remaining acoustic field on the probe light is negligible (an assumption to be later justified by numerical simulation), we theorize that Eq. (5) can be generalized to represent the power arriving at the detector at any moment $t > 0$ by substituting the constant boundary of integration, with a time-dependent term:

$$P_{\text{detected}}(t > t_0) = P_{s0}\exp[I_p \int_0^{L-(v_g t/2)} G(z')dz'] \qquad (6)$$

The 1/2 factor appearing in the variable term accounts for the round-trip time inherent to any scheme in which the pump and probe counter-propagate. Intuitively, one can see that the monotonously-decreasing Stokes power detected at the time period succeeding the pump light shut-down, given in Eq. (6), is none other than a backwards trace of the spatial profile of amplification the probe has been undergoing under the CW-like pump, prior to its extinction. Accordingly, the local slope at any point along this traced profile directly describes the local Brillouin gain existing at that point. Stated more rigorously - by taking the derivative, and after some rearrangement of terms, we arrive at:

$$\frac{d[\ln(P_{\text{detected}})]}{dt} = \left(-\frac{v_g I_p}{2}\right)G\left(L - \frac{v_g}{2}t\right) \propto G\left(L - \frac{v_g}{2}t\right) \qquad (7)$$

Hence, the derivative of the logarithm of the probe signal is linearly proportional to the Brillouin gain along the fiber, mapped through the standard round-trip time relation. The spatial resolution expected by this treatment is hypothetically infinite, because it assumes an ideal modulation scheme which shuts down the pump power instantaneously. In practice, the pump wave will have a finite fall-time, hence its falling edge - which serves as the fundamental interrogation element of the sensor - has a finite spatial width. Therefore, the limiting parameter for the spatial resolution achievable with the GPT technique is the fall-time of the pump modulation (which we shall denote t_{fall}), through the relation:

$$\Delta z_{\text{resolvable}} = \left(v_g/2\right)t_{\text{fall}} \qquad (8)$$

Lastly, we recall the mapping procedure illustrated above takes place at some specific difference of the pump and probe optical frequencies, i.e., at a fixed $\Omega_B - \omega_p + \omega_s$ value. Complete knowledge of the Brillouin frequency at each sensing point is obtained by discretely sweeping (preferably the probe) frequency and reiterating the measurement process for every frequency point, in order to reconstruct a good representation of the Brillouin gain spectrum.

4. Numerical Simulation

Validation of the proposed method was sought by straight-forward numerical integration in the time domain of the fundamental SBS Eq. (1)-(3). The results indeed verified the predictions given by the theoretical discussion. A demonstration for a specific case of a sensing fiber 10m long, with a 20cm section distinguished from the background by having a Brillouin frequency offset of 30MHz located exactly at its middle, is given in Fig. 2 as a mapping of the Brillouin gain vs. location and frequency. The demonstration also simulated an implementation of the "Dark Pulse" technique of [2] upon the same test fiber. The fall-time of the GPT pulse was modeled to be 100ps, and the dark pulse was simulated as a square pulse with a 100ps width. This is a more than fair comparison, since in practice, the pump modulation scheme that would be able to produce the modeled GPT pulse (i.e., one having a rise/fall time of 100ps), could not produce a square pulse of identical width, but only wider square pulses. The natural Brillouin linewidth was modeled as 30MHz. At the top of Fig. 2 are the results obtained using the proposed GPT method. Clearly, the sharpness of details in the mapping indicates high spatial resolution, in agreement with the prediction of Eq. (8), which for the 0.1ns fall-time corresponds to 1cm. Furthermore, the 30MHz frequency difference at the offset section is correctly recovered, because the spectral profile of the Brillouin response faithfully represents the local natural Brillouin gain spectrum, both at the background fiber and at the offset fiber section. At the bottom of Fig. 2, the results of the dark pulse can be seen to exhibit similarly sharp details with cm-order spatial resolution, but the spectral behavior of the response at the offset section greatly deviates from the desired curve that should be

centered around the detuning value of 30MHz. This is due to the effect of the "secondary echo" which arises in the dark pulse scheme as an acoustic response to the event of the pump power's re-appearance, occurring at the end of the pulse. During the time the pulse passes a certain point, the pre-excited acoustic field there experiences some relaxation. The recovery from this relaxation begins once the pulse has departed that certain location, therefore it is manifested in the detected signal as a "phantom" Brillouin response emanating from adjacent points in the fiber. Thus, the response appearing at the offset section for detuning values around zero can be seen to represent not the true local Brillouin gain, but rather undesired contributions made by the neighboring sections, those belonging to the background fiber. In the GPT scheme, contrastingly, once the pump power vanishes from a certain point it does not re-appear there, hence the slow relaxation of the acoustic field bears no effect upon the probe signal, and no "secondary echoes" exist.
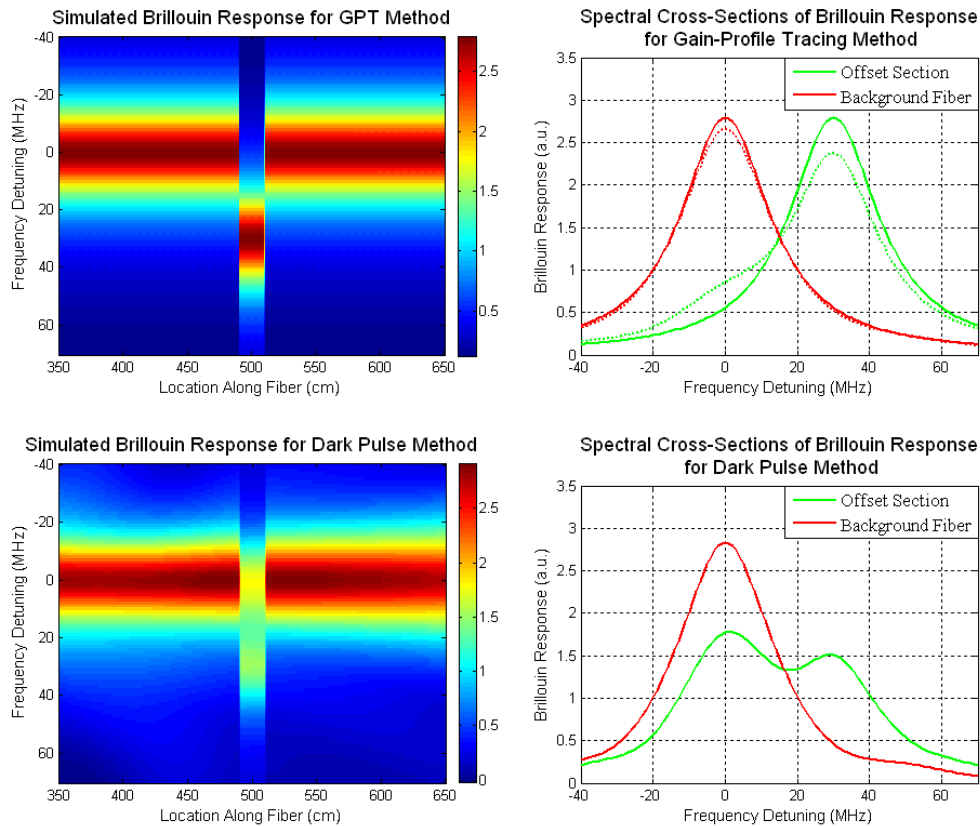

Fig. 2. Simulated Brillouin Gain mapping, vs. location and frequency, for: (top) the proposed GPT method, (bottom) the referenced dark pulse method. The frequency axis is plotted relative to the background fiber, so that at zero frequency detuning, the SBS response of the background fiber is maximum. On the left side full mappings are illustrated, indicated by color axis (in arbitrary units). On the right are cross-sections of these mappings taken at two exemplary locations – one at the offset fiber section, and one located outside this section. The dotted lines at the top right figure show the Brillouin response obtained by the GPT method at the same locations with a pump modulation having a finite extinction ratio of 15dB.

We conclude the numerical section by addressing the issue of the finite extinction ratio (ER) the pump modulation would exhibit in any real-world implementation of the proposed method. It can be expected that leakage of pump light through the modulator after the switch-off would give rise to some undesired effects upon the sensing, since ideally, we would prefer to have the SBS interaction cease completely after the shut-down event. The feature of a finite

ER was added to the modeled pump, and simulations were run for several scenarios with varying ER values. The results confirmed that for realistic values of the ER (over 10dB), deviations from the idealized theory presented earlier are very small. Such results, obtained for a simulated pump-pulse of 15dB extinction ratio (commonly, even better values of 20-30 dB are achieved in practice), are shown at the top right of Fig. 2 by the dotted lines. As can be seen, the deviation from the results obtained for an idealized pump-pulse of infinite extinction (indicated by the solid lines) is minor, and the frequency at which the spectral response curve attains its maximum remains practically the same.

5. Experiment and Discussion

The distributed Brillouin sensor configuration of Fig. 3 was used for experimental validation. A sample fiber was prepared by inserting (i.e., splicing) short segments of fiber with a Brillouin frequency of 10.875GHz, into a 4m long fiber differing by 13MHz (i.e., with Brillouin frequency of 10.862GHz). The light of the laser source, at 1550nm, was split into two branches, serving as pump and probe waves. The pump wave was modulated by a square-wave signal featuring a long "on time" of $0.5\mu s$ (long enough for the pre-excitation of the SBS amplification in the fiber to reach a steady state), and a markedly short fall-time of 100ps. The pulse repetition period was set to $2\mu s$ (hence a 25% duty-cycle). The pump light was amplified to 30dBm before being launched into the sample under test. The CW probe light, with an optical frequency smaller than that of the pumping light by roughly the Brillouin frequency, was generated through intensity modulation (see [9] for example) followed by suppression of the carrier and the undesired sideband, performed by the FBG. The probe light was then launched into the sensing fiber, with an initial optical power of 6dBm, and detected at the other end (after experiencing SBS gain) by a high-speed photo-receiver. The role of the FBG located just before the receiver was to filter out some of the optical noise sources, such as the Rayleigh backscatter of the pump light. A high bandwidth oscilloscope monitored the detected power, averaging each fiber trace 1000 times. The probe frequency was step-swept across the relevant spectral range of 10.84GHz to 10.89GHz.
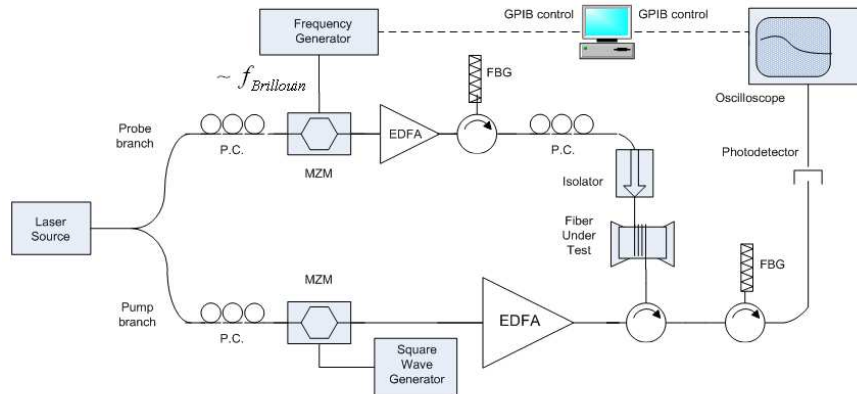

Fig. 3. Experimental setup. Both MZMs (Mach-Zehnder Modulators) are amplitude modulators. PC stands for Polarization Controller, EDFA for Erbium-Doped Fiber Amplifier, FBG for Fiber Bragg Grating.

Results are given firstly for the case of a sample fiber with an inserted offset segment of 5cm length, providing a preliminary demonstration of the sensing method's validity. Figure 4 illustrates the various stages of data acquisition and analysis performed in order to obtain the results. At the top left are shown two exemplary fiber traces (i.e., time-domain probe signals detected immediately after the pump shut-down event), as captured by the oscilloscope. The display of these originally time-domain signals as functions of location is based upon the

standard round-trip time relation $z = v_g t/2$. One trace was detected at a frequency shift in-tune with the Brillouin frequency of the background fiber, and the other was detected at the shift tuned to the Brillouin frequency of the offset segment. The slopes of the signals, which - according to the predictions of the theoretical discussion - represent local Brillouin gain, can be seen to be large only at those locations where the fiber is "tuned" to the frequency shift.
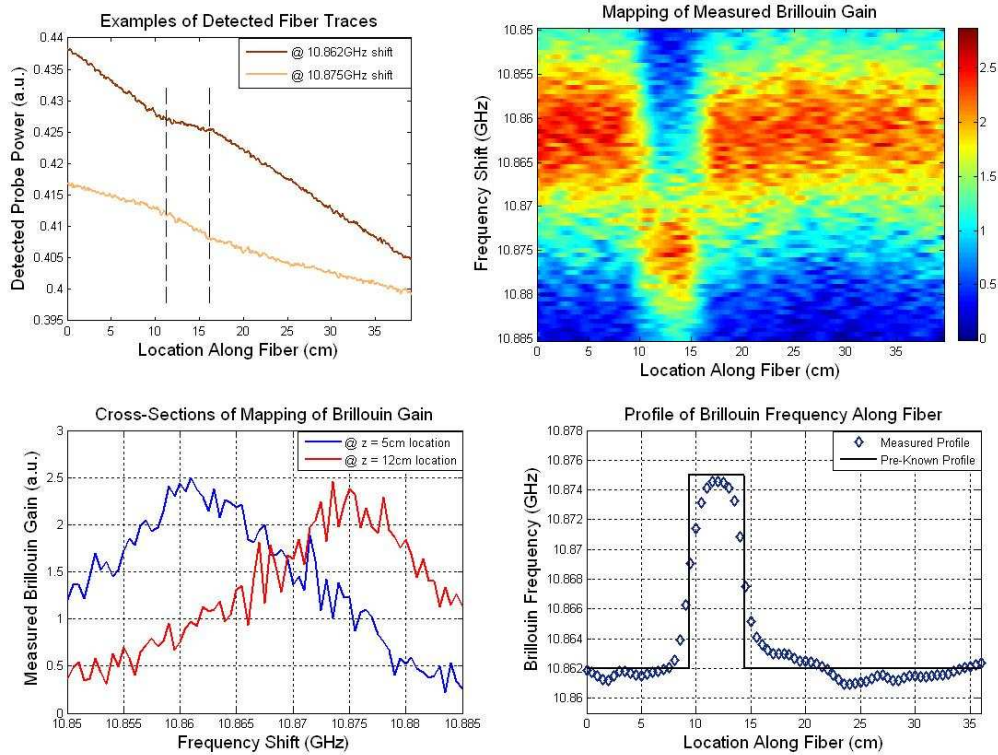

Fig. 4. Processed experimental data for the case of a 5cm offset segment. Top left – fiber traces as acquired by the oscilloscope, prior to any processing. The dashed lines mark the offset segment in the fiber. Top right – Brillouin gain mapping obtained by trace differentiation, indicated by color axis (in arbitrary units). The frequency shift step size is 0.5MHz. Bottom left – spectral gain curves obtained by taking cross-sections of the gain mapping at exemplary locations. Bottom right - final results, obtained by estimating per each location point the center of the spectral gain-curve. Each point represents 0.5cm of fiber.

Next, each trace was processed according to Eq. (7) in order to resolve the absolute Brillouin gain along the fiber, and by placing the data from all the sampled frequencies side by side, the mapping of the Brillouin gain vs. both location and frequency shift was produced - shown at top right. We note that the achievable spatial resolution was limited by the given pump-modulation scheme to 1cm (as dictated by Eq. (8) for a pump fall-time of 100ps), while the probe signals were acquired with a sampling frequency considerably higher, specifically 14 points/cm. Consequentially, had the signal differentiation of Eq. (7) been realized by straight-forward derivation, the results would represent data sampled with excessive bandwidth, and heavily burdened by noise (because the difference between any two adjacent sampled points would yield information at a spatial frequency well over the maximal frequency we can hope to resolve). Therefore, the differentiation was realized by performing linear fits to the trace with a moving 2cm window, meaning that the local derivative at any location point was taken to be the slope of a linear fit done on a 2cm-long interval of the trace centered on that point. Obviously, such processing is a form of smoothening, which overcomes noise at the expense of reducing spatial resolution; the width of the moving

window represents the smallest feature still resolvable in the processed data, but as this width is increased, noise is spatially averaged over a longer interval, and is thus diminished. Data processing was attempted with different window sizes, eventually the 2cm window width was chosen as the optimal achievable compromise between the intent of maximizing the spatial resolution, and the necessity of smoothening the data to allow the presentation of intelligible results. Moving on to the bottom left of Fig. 4, the process of evaluating the Brillouin frequency at any given location in the fiber is demonstrated. Two exemplary spectral cross-sections of the gain mapping are plotted, one taken at a point located in the background fiber, the other taken at a point within the offset segment. Clearly, the cross-sections give a good reproduction of the expected Brillouin Gain Spectrum at each location, in agreement with the simulation predictions shown in Fig. 2. Lastly, by fitting the spectral gain curve per each location point to the desired bell-shaped model of Eq. (4), and identifying the central frequency of the fit as the local Brillouin frequency, the fiber's spatial Brillouin frequency profile was evaluated – illustrated at bottom right.

The next experiment was conducted using the same set-up, and a sample fiber with a shorter inserted offset segment, of 2cm length, serving as a test-case for gauging the method's achievable spatial resolution. The results are given in Fig. 5 in the same manner of Fig. 4, with the two demonstrative left-side plots omitted, since the methods of processing and analyzing the data have not changed and their explanation need not be repeated. As visible in the gain mapping on the left, the offset segment can still be clearly distinguished from the background fiber. In the Brillouin frequency profile (right side of the figure) the 2cm offset is seen to be detected with, approximately, the correct spatial length, but the outline is quite smoothened at the borders (the transition between the two frequencies is gradual). This suggests that the lower bound of the spatial resolution has been reached in the measurement. As mentioned earlier, the theoretical lower bound for the spatial resolution is, for the employed pump pulsing, lower – about 1cm; however, further approach of this bound would require some reduction of the detected noise power, so as to allow data-processing using a smaller spatial window. Such mitigation of measured noise can possibly be achieved by further optimization of the optical filtering, or by lengthening the averaging performed for each acquired trace. We further note that the mean error of the final Brillouin frequency measurement is 1-2MHz, as seen, in the spatial profile plotted on the right, as discrepancies between the measured data and the pre-known profile. This error can probably be lowered by increasing the number of sampled frequency points, thus improving the accuracy with which the spectral gain curves are obtained and analyzed – provided longer acquisition times can be tolerated.
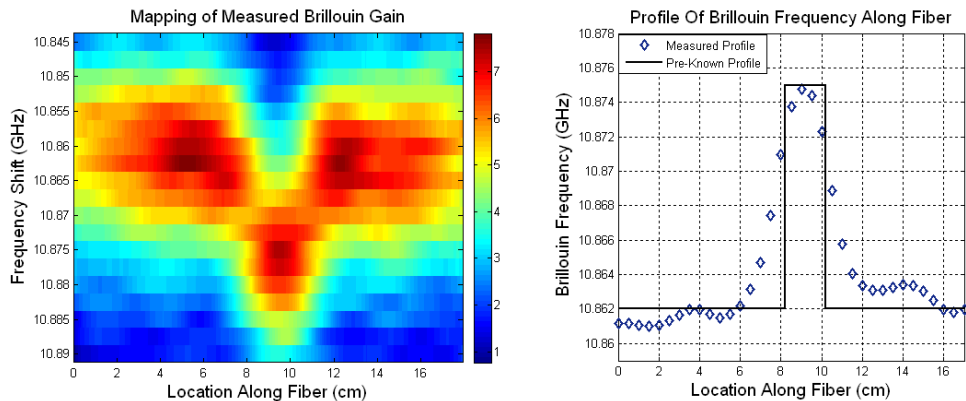

Fig. 5. Processed experimental data for the case of a 2cm offset segment. Left - Brillouin gain mapping obtained by trace differentiation, indicated by color axis (in arbitrary units). The frequency shift step size is 2.5MHz. Right - final results, obtained by estimating per each location point the center of the spectral gain-curve. Each point represents 0.5cm of fiber.

6. Conclusion

In this paper we have proposed and demonstrated a novel BOTDA distributed sensor exhibiting cm-order resolution, based on a direct gain-profile tracing scheme. The sensor utilizes the common pre-excitation approach, but is unique in the fact that no interrogating pulse which physically interacts with the acoustic waves is launched. This allows the modulation of the pump to be simplified to a single-transition shut-down, therefore bringing the lower bound for theoretically achievable spatial resolution to the typical fall-time of the modulating system. It should be noted, that the total sensing distance over which the proposed technique is applicable (although this subject has yet to be fully investigated in future work) can be predicted to be limited, since the need to generate Brillouin gain under CW-like conditions along the entire fiber gives rise to several undesired phenomena, such as pump depletion and spontaneous Brillouin scattering. On the other hand, this limiting feature is shared by most other sensing techniques based upon pre-excitation of the acoustic field in the fiber, and can be overcome only by implementing a pulse-pair technique, where each fiber trace is produced by subtracting two separate measured signals taken at the same frequency shift (see [4,5]). The advantage, therefore, featured by the proposed Gain-Profile Tracing technique, for the applicable range of sensing lengths, is the ability to measure the desired Brillouin response with just one trace taken per frequency point. To the best of our knowledge, the results reported above, where a Brillouin-frequency difference of 13MHz was resolved with a spatial resolution of 2cm, demonstrate the best spatial resolution reported so far for a sensing scenario in which the resolved frequency separation is smaller than the natural Brillouin line width.

Acknowledgments